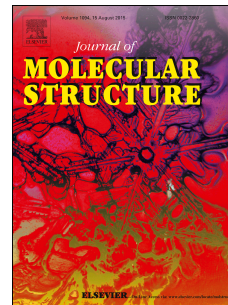


Accepted Manuscript

Crystal and molecular structure studies of (Z)-N-methyl-C-4-substituted phenyl nitrones by XRD, DFT, FTIR and NMR methods

Jamal Lasri, Naser Eltahir Eltayeb, Matti Haukka, Yousef Alghamdi



PII: S0022-2860(16)30888-2

DOI: [10.1016/j.molstruc.2016.08.058](https://doi.org/10.1016/j.molstruc.2016.08.058)

Reference: MOLSTR 22884

To appear in: *Journal of Molecular Structure*

Received Date: 11 June 2016

Revised Date: 17 August 2016

Accepted Date: 18 August 2016

Please cite this article as: J. Lasri, N.E. Eltayeb, M. Haukka, Y. Alghamdi, Crystal and molecular structure studies of (Z)-N-methyl-C-4-substituted phenyl nitrones by XRD, DFT, FTIR and NMR methods, *Journal of Molecular Structure* (2016), doi: 10.1016/j.molstruc.2016.08.058.

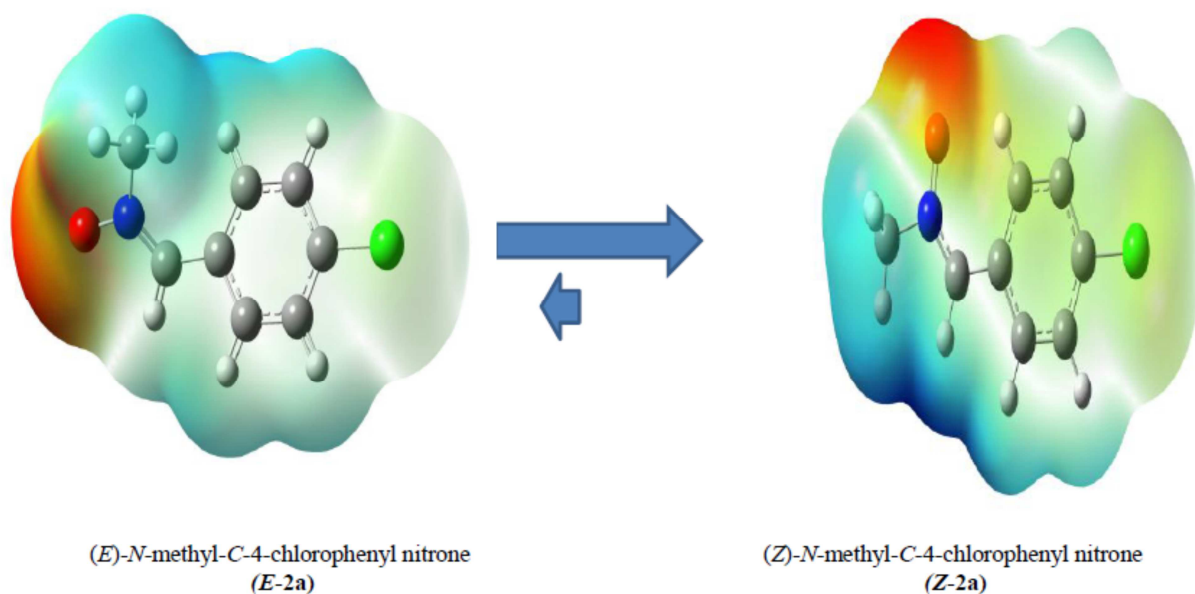
This is a PDF file of an unedited manuscript that has been accepted for publication. As a service to our customers we are providing this early version of the manuscript. The manuscript will undergo copyediting, typesetting, and review of the resulting proof before it is published in its final form. Please note that during the production process errors may be discovered which could affect the content, and all legal disclaimers that apply to the journal pertain.

Crystal and molecular structure studies of (*Z*)-*N*-methyl-*C*-4-substituted phenyl nitrones by XRD, DFT, FTIR and NMR methods

Jamal Lasri*, Naser Eltaher Eltayeb, Matti Haukka, Yousef Alghamdi

GRAPHICAL ABSTRACT

New *N*-methyl-*C*-4-substituted phenyl nitrones have been synthesized and characterized by elemental analyses, FTIR, NMR and X-ray diffraction. The relative stabilities of their two possible isomers (*E* and *Z*) have been investigated using the B3LYP/6-311++G(d,p).



Crystal and molecular structure studies of (*Z*)-*N*-methyl-*C*-4-substituted phenyl nitrones by XRD, DFT, FTIR and NMR methods

Jamal Lasri^{a,*}, Naser Eltaher Eltayeb^a, Matti Haukka^b, Yousef Alghamdi^a

^a Department of Chemistry, Rabigh College of Science and Arts, P.O. Box 344, King Abdulaziz University, Jeddah, Saudi Arabia

^b University of Jyväskylä, Department of Chemistry, P.O. Box 35, FI-40014 University of Jyväskylä, Finland

* Corresponding author at: Department of Chemistry, Rabigh College of Science and Arts, P.O. Box 344, King Abdulaziz University, Jeddah, Saudi Arabia. E-mail address: jlasri@kau.edu.sa (J. Lasri).

ABSTRACT

(*Z*)-*N*-methyl-*C*-4-substituted phenyl nitrones $^{\ominus}\text{O}^{\oplus}\text{N}(\text{Me})=\text{C}(\text{H})\text{R}$ (**Z-2a** R = 4-ClC₆H₄, **Z-2b** R = 4-NO₂C₆H₄, **Z-2c** R = 4-CH₃OC₆H₄) were synthesized and characterized by elemental analyses, FTIR, ¹H, ¹³C and DEPT-135 NMR spectroscopy and also by single crystal X-ray diffraction (in the case of **Z-2a** and **Z-2b**). The geometries of the nitrone molecules **Z-2a**, **Z-2b** and **Z-2c** and their *E*-isomers; (*E*)-*N*-methyl-*C*-4-chlorophenyl nitrone **E-2a**, (*E*)-*N*-methyl-*C*-4-nitrophenyl nitrone **E-2b** and (*E*)-*N*-methyl-*C*-4-methoxyphenyl nitrone **E-2c** were optimized using density functional theory (DFT) at the B3LYP/6-311++G(d,p) level of theory. The theoretical vibrational frequencies obtained by DFT calculations are in good agreement with the experimental values. The electronics structures were described in terms of the distribution of the highest occupied molecular orbital (HOMO) and the lowest unoccupied molecular orbital (LUMO). Gauge independent atomic orbital (GIAO) method was used to calculate the NMR spectra, the correlation between the calculated and experimental chemical shifts is mostly in the range of 0.94-0.97 for ¹H, whereas, the correlation for ¹³C is 0.99. Thermodynamics study showed that the *Z*-isomer is favoured than *E*-isomer with energy barrier of 7.1, 7.2 and

7.1 Kcal/mol for **Z-2a**, **Z-2b** and **Z-2c**, respectively. The abundance of the most stable species *Z*-isomers is equal to 99.99% for all three compounds at 298 K in gas phase.

Keywords: (*Z*)-*N*-methyl-*C*-4-substituted phenyl nitrones; Single crystal X-ray; NMR; DFT; B3LYP.

1. Introduction

Acyclic and cyclic nitrones have been extensively reviewed in organic chemistry [1,2], they have been utilized for the preparation of numerous natural products with interesting biological activities [3]. These products are found to act as an important key step in the incorporation of multiple stereo-centers *via* 1,3-dipolar cycloaddition reactions [4]. On this regards, nitrone moiety is found to possess pharmacological applications [5] and form an important part of the molecular structure of many drugs. Some nitrones have biological activities in several animal models [6,7]. Ageing, Alzheimer and Parkinsons diseases as well as cancer development are very known to have improved levels of free radicals and oxidative stress. Furthermore, nitrones have also anticancer activities in various experimental cancer models and have potential as therapeutics in various cancers [8]. On the other hand, the combination of antioxidants with nitrones has shown a synergistic effect to inhibit the acute acoustic noise induced hearing loss [9]. Nitrone compounds are also of industrial importance in the corrosion of metals / alloys in acidic media (organic) as most carboxylic acids are utilized as building blocks in a variety of industrial processes such as drugs, fibers and plastics [10-13].

In this work, (*Z*)-*N*-methyl-*C*-4-substituted phenyl nitrones $^-\text{O}^+\text{N}(\text{Me})=\text{C}(\text{H})\text{R}$ (**Z-2a** R = 4-ClC₆H₄, **Z-2b** R = 4-NO₂C₆H₄, **Z-2c** R = 4-CH₃OC₆H₄) were synthesized and characterized by elemental analyses, FTIR, ¹H, ¹³C and DEPT-135 NMR spectroscopy and also by single crystal X-ray diffraction (in the case of **Z-2a** and **Z-2b**). Moreover, we were interested to look for the correlations between the experimental results and the computational calculations based on density functional theory (DFT) of electronic, spectroscopic properties.

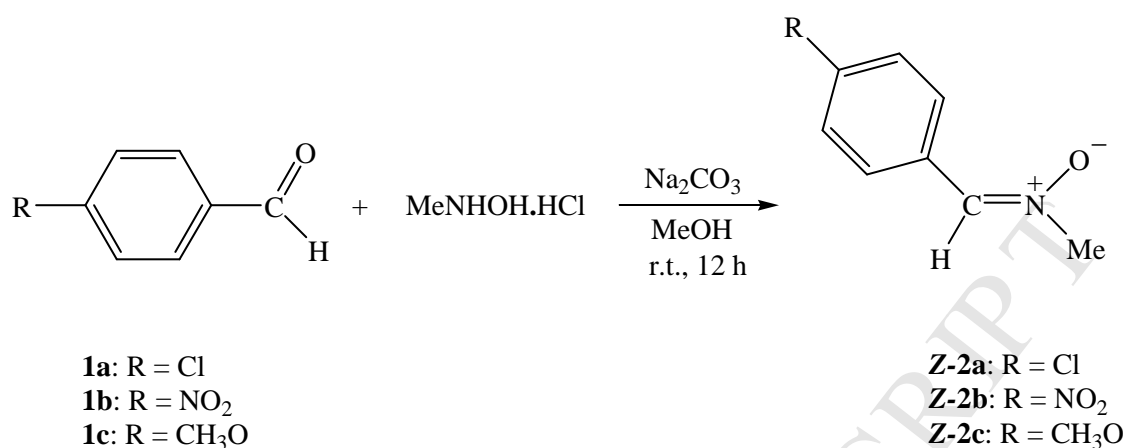
2. Experimental Section

2.1. Material and instrumentation

Solvents and reagents were obtained from commercial sources (Aldrich) and used as received. C, H and N elemental analyses were carried out by the Microanalytical Service of the King Abdulaziz University. ^1H , ^{13}C and DEPT-135 NMR spectra (in CDCl_3) were measured on Bruker Avance III HD 600 MHz (AscendTM Magnet) spectrometer at ambient temperature. ^1H , ^{13}C and DEPT-135 chemical shifts (δ) are expressed in ppm relative to TMS. Infrared spectra ($400\text{-}4000\text{ cm}^{-1}$) were recorded on an Alpha Bruker FT-IR instrument in KBr pellets.

2.2. Synthesis of (Z)-N-methyl-C-4-substituted phenyl nitrone **Z-2a**, **Z-2b** and **Z-2c**

To a solution of *N*-methylhydroxylamine hydrochloride (1.00 g, 11.97 mmol) in MeOH (4 mL) was added sodium carbonate (0.63 g, 5.98 mmol). The reaction mixture was stirred at room temperature for 5 min. 4-Chlorobenzaldehyde **1a** (1.53 g, 10.88 mmol), 4-nitrobenzaldehyde **1b** (1.64 g, 10.88 mmol) or 4-methoxybenzaldehyde **1c** (1.48 g, 10.88 mmol) was added and the reaction mixture was stirred for 12 h. The precipitate formed was then filtered off and the filtrate was evaporated *in vacuo*. The solid was then dissolved in CHCl_3 resulting in the precipitation of NaCl, and it was filtered off and the CHCl_3 was then removed *in vacuo*. The final product was washed with Et_2O to afford the pure (Z)-*N*-methyl-C-4-chlorophenyl nitrone **Z-2a**, (Z)-*N*-methyl-C-4-nitrophenyl nitrone **Z-2b** or (Z)-*N*-methyl-C-4-methoxyphenyl nitrone **Z-2c**, respectively, in *ca.* 90% yield (Scheme 1).



Scheme 1. Synthesis of *N*-methyl-*C*-4-substituted phenyl nitrones **Z-2a**, **Z-2b** and **Z-2c**.

⁻O⁺N(Me)=C(H)(4-ClC₆H₄) (Z-2a)

Yield: 91%. IR (cm⁻¹): 1655 (C=N). ¹H NMR (CDCl₃), δ: 3.77 (s, 3H, CH₃N), 7.28 (s, 1H, C(H)=N), 7.28 (d, 2H, *J*_{HH} = 8.6 Hz, CH_{ar}), 8.09 (d, 2H, *J*_{HH} = 8.6 Hz, CH_{ar}). ¹³C NMR (CDCl₃), δ: 54.4 (CH₃N), 128.6 (CH_{aromatic}), 128.9 (C_{aromatic}), 129.5 (CH_{aromatic}), 134.0 (C(H)=N), 135.6 (C_{aromatic}). DEPT-135 NMR (CDCl₃), δ: 54.4 (CH₃N), 128.6 (CH_{aromatic}), 129.5 (CH_{aromatic}), 134.0 (C(H)=N). Anal. Calc. for C₈H₈NOCl: C, 56.65; H, 4.75; N, 8.26. Found: C, 56.77; H, 4.91; N, 8.15%.

⁻O⁺N(Me)=C(H)(4-NO₂C₆H₄) (Z-2b)

Yield: 90%. IR (cm⁻¹): 1598 (C=N). ¹H NMR (CDCl₃), δ: 3.98 (s, 3H, CH₃N), 7.54 (s, 1H, C(H)=N), 8.28 (d, 2H, *J*_{HH} = 8.8 Hz, CH_{ar}), 8.40 (d, 2H, *J*_{HH} = 8.8 Hz, CH_{ar}). ¹³C NMR (CDCl₃), δ: 55.1 (CH₃N), 123.8 (CH_{aromatic}), 128.7 (CH_{aromatic}), 133.1 (C(H)=N), 136.0 (C_{aromatic}), 147.9 (C_{aromatic}). DEPT-135 NMR (CDCl₃), δ: 55.1 (CH₃N), 123.8 (CH_{aromatic}), 128.7 (CH_{aromatic}), 133.1 (C(H)=N). Anal. Calc. for C₈H₈N₂O₃: C, 53.33; H, 4.48; N, 15.55. Found: C, 53.48; H, 4.17; N, 15.30%.

$\text{O}^+\text{N}(\text{Me})=\text{C}(\text{H})(4\text{-CH}_3\text{OC}_6\text{H}_4)$ (Z-2c**)**

Yield: 89%. IR (cm^{-1}): 1603 (C=N). ^1H NMR (CDCl_3), δ : 3.75 (s, 3H, CH_3O), 3.76 (s, 3H, CH_3N), 6.86 (d, 2H, $J_{\text{HH}} = 8.9$ Hz, CH_{ar}), 7.25 (s, 1H, C(H)=N), 8.14 (d, 2H, $J_{\text{HH}} = 8.9$ Hz, CH_{ar}). ^{13}C NMR (CDCl_3), δ : 53.8 (CH_3O), 55.3 (CH_3N), 113.8 ($\text{CH}_{\text{aromatic}}$), 123.4 ($\text{C}_{\text{aromatic}}$), 130.5 ($\text{CH}_{\text{aromatic}}$), 135.2 (C(H)=N), 161.1 ($\text{C}_{\text{aromatic}}$). DEPT-135 NMR (CDCl_3), δ : 53.8 (CH_3O), 55.3 (CH_3N), 113.8 ($\text{CH}_{\text{aromatic}}$), 130.5 ($\text{CH}_{\text{aromatic}}$), 135.2 (C(H)=N). Anal. Calc. for $\text{C}_9\text{H}_{11}\text{NO}_2$: C, 65.44; H, 6.71; N, 8.48. Found: C, 65.56; H, 6.88; N, 8.35%.

2.3. X-ray crystallography

For the X-ray structure determinations; X-ray-quality single crystal of (*Z*)-*N*-methyl-*C*-4-chlorophenyl nitron **Z-2a** and (*Z*)-*N*-methyl-*C*-4-nitrophenyl nitron **Z-2b** was obtained by slow evaporation from chloroform. The crystals of **Z-2a** and **Z-2b** were immersed in cryo-oil, mounted in a MiTeGen loop and measured at 120–170 K. The X-ray diffraction data were collected on a Bruker KappaApex II or an Agilent Technologies Supernova using Mo $K\alpha$ radiation ($\lambda = 0.70173$ Å). The Denso/Scalepack [14] or CrysAlisPro [15] program packages were used for cell refinements and data reductions. The structures were solved by charge flipping method using the SUPERFLIP [16] program. A multi-scan absorption correction based on equivalent reflections (SADABS, [17] CrysAlisPro) was applied to all data. Structural refinements were carried out using SHELXL2014 [18]. The hydrogen atoms were positioned geometrically and constrained to ride on their parent atoms, with C–H = 0.95–0.98 Å and $U_{\text{iso}} = 1.2\text{--}1.5 U_{\text{eq}}$ (parent atom). The crystallographic details are summarized in Table 1. CCDC numbers 1482396 and 1482397 contain the supplementary crystallographic data for this paper. These data can be obtained free of charge from The Cambridge Crystallographic Data Centre *via* www.ccdc.cam.ac.uk/data_request/cif.

Table 1. Crystal Data.

	Z-2a	Z-2b
Empirical formula	C_8H_8ClNO	$C_8H_8N_2O_3$
Fw	169.60	180.16
Temp (K)	170(2)	120(2)
λ (Å)	0.71073	0.71073
Cryst syst	<i>Monoclinic</i>	<i>Orthorhombic</i>
Space group	$P2_1/c$	$Pbc2_1$
a (Å)	11.6636(5)	11.70106(16)
b (Å)	9.7903(4)	10.94074(16)
c (Å)	7.3574(3)	2.3169(2)
β (deg)	107.602(2)	90
V (Å ³)	800.81(6)	1576.78(4)
Z	4	8
ρ_{calc} (Mg/m ³)	1.407	1.518
μ (Mo K α) (mm ⁻¹)	0.413	0.119
No. reflns.	11951	38660
Unique reflns.	2363	5981
GOOF (F^2)	1.145	1.120
R_{int}	0.0504	0.0287
$R1^a$ ($I \geq 2\sigma$)	0.0582	0.0350
$wR2^b$ ($I \geq 2\sigma$)	0.0951	0.1027

$$^a R1 = \sum ||F_o| - |F_c|| / \sum |F_o|. \quad ^b wR2 = [\sum [w(F_o^2 - F_c^2)^2] / \sum [w(F_o^2)^2]]^{1/2}.$$

2.4. Computational methods

Molecular electronic structure calculations were performed using the density functional theory (DFT). The DFT calculations were performed by Becke's three-parameter exchange functional with Lee–Yang–Parr (LYP) correlation functional. Gaussian 09 software [19] were used to performed full geometry optimizations of the compounds at the B3LYP level of theory using an 6-311++G (d,p) basis set. The optimization was confirmed with absence of negative frequency. The gauge-independent atomic orbital (GIAO) method was used at the B3LYP/6-311++G (d,p) level of theory to calculate the NMR chemical shifts with Polarizable Continuum Model (PCM). The softwares; Chemcraft [20] and Veda 4 [21] were used to analysis of Gaussian 09 output files.

3. Results and discussion

In this work, the molecular structure of (*Z*)-*N*-methyl-*C*-4-chlorophenyl nitrone **Z-2a**, (*Z*)-*N*-methyl-*C*-4-nitrophenyl nitrone **Z-2b** and (*Z*)-*N*-methyl-*C*-4-methoxyphenyl nitrone **Z-2c** have been studied theoretically by DFT and experimentally by XRD, FTIR and NMR methods. The *E*-isomers; (*E*)-*N*-methyl-*C*-4-chlorophenyl nitrone **E-2a**, (*E*)-*N*-methyl-*C*-4-nitrophenyl nitrone **E-2b** and (*E*)-*N*-methyl-*C*-4-methoxyphenyl nitrone **E-2c** have been studied theoretically using DFT method.

3.1. Crystal structure

The molecular structure and numbering of (*Z*)-*N*-methyl-*C*-4-chlorophenyl nitrone **Z-2a** and (*Z*)-*N*-methyl-*C*-4-nitrophenyl nitrone **Z-2b** are shown in Fig. 1 and Fig. 2, and the crystal packing along the *b* axis is presented in Fig. 3 and Fig. 4, respectively. Table 1 showed crystal data and structure refinement for compounds **Z-2a** and **Z-2b**. Table 2 lists some selected bond lengths, bond angles and selected torsion angles.

Crystal structure of (Z)-N-methyl-C-4-chlorophenyl nitrone Z-2a

In the (*Z*)-*N*-methyl-*C*-4-chlorophenyl nitrone **Z-2a**, the benzene ring is planar. The chloride atom, C11, deviates from this plane by 0.010 (1) Å while the methyl C atom, C7, is out of the plane by 0.031 (2) Å. The chains O1/N1/C7/C1 and C8/N1/C7/C1 have torsional angles -2.0 (3)° and 176.81 (19)°, respectively. The bond lengths indicate double-bond character for the C7=N1 [1.306 Å] bond and single-bond character for the C8—N1 [1.474 Å] and O1—N1 [1.294 Å] bonds. An intramolecular C(6)—H(6)⋯O1 hydrogen bond is observed (Fig. 1). This interaction generates an *S*(6) ring motif.

In the crystal, molecules are linked through intermolecular C8—H8⋯O1 [symmetry code: $1-x, 1/2+y, 3/2-z$] and C7—H7⋯O1 [$x, 1/2 - y, -1/2 + z$] hydrogen bonds into supramolecular chains propagating along the *b* axis direction (Fig. 3). C—H⋯ π interactions are present C(5)—H(5)⋯ Cg(1) [symmetry code: $(X, 1/2-Y, 1/2+Z)$] and C(8)—H(8B)⋯Cg(1) [symmetry code: $1-X, 1-Y, 2-Z$], with H⋯Cg 2.73 Å and 2.75 Å, respectively. Where Cg(1) is the centroid of the ring represented by C(1)—C(6).

Crystal structure of (Z)-N-methyl-C-4-nitrophenyl nitrone Z-2b

In the (*Z*)-*N*-methyl-*C*-4-nitrophenyl nitrone **Z-2b**, the benzene ring is planar. The nitrogen atom, N₂, deviates from this plane by 0.014(1) Å [0.011(1) Å in molecule B], while the methyl C atom, C8, is out of the plane by 0.069(2) Å [-0.026(2) Å in molecule B]. The chains O1/N1/C7/C6 and C8/N1/C7/C6 have torsional angles 0.7 (3)° [-1.0(2) in molecule B] and -179.73 (15)° [-179.75(14) in molecule B], respectively. The bond lengths indicate double-bond character for the C7=N1 [1.311 Å] bond and single-bond character for the C8—N1 [1.475 Å] and O1—N1 [1.290 Å] bonds as same as for molecule B.

An intramolecular C(5)—H(5)⋯O1 hydrogen bond is observed in molecule A and B (Fig. 2). This interaction generates an *S*(6) ring motif. In the crystal, molecules are linked through intermolecular C7—H7A⋯O1 [symmetry code: $1-x, 1/2+y, z$], C2—H2A⋯O3 [symmetry code: $-x, 1/2+y, z$] and C4—H4A⋯O2 [symmetry code: $-x, -1/2+y, z$] for molecule A and C7B—H7BA⋯O1B [symmetry code: $-x, -1/2+y, z$], C2B—H2BA⋯O3B [symmetry code: $1-x, -1/2+y, z$] and C4B—H4BA⋯O2B [symmetry code: $1-x, 1/2+y, z$]

for molecule B, hydrogen bonds into supramolecular sheets propagating along the *b* axis direction (Fig. 4). C—H... π interaction is absent and the shortest centroid–centroid separations being 4.004 Å for aromatic π – π stacking between *Cg*(1)–*Cg*(2) [symmetry code: X,Y,Z], Where *Cg*(1) is the centroid of the ring represented by C(1)—C(6) and *Cg*(2) is the centroid of the ring represented by C(1B)—C(6B).

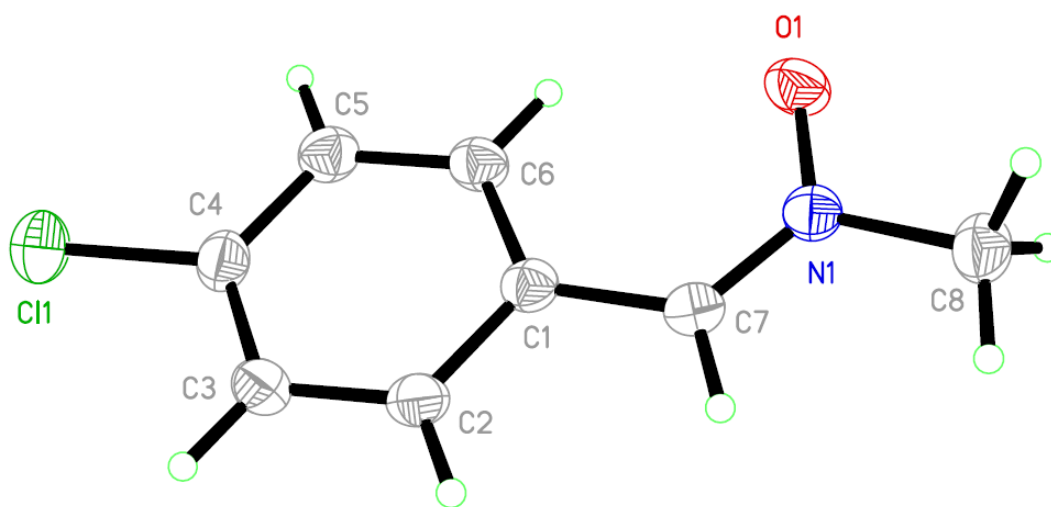


Fig. 1. ORTEP drawing of (*Z*)-*N*-methyl-*C*-4-chlorophenyl nitrone **Z-2a** showing the atom numbering scheme and 30% probability displacement ellipsoids of non-H atoms.

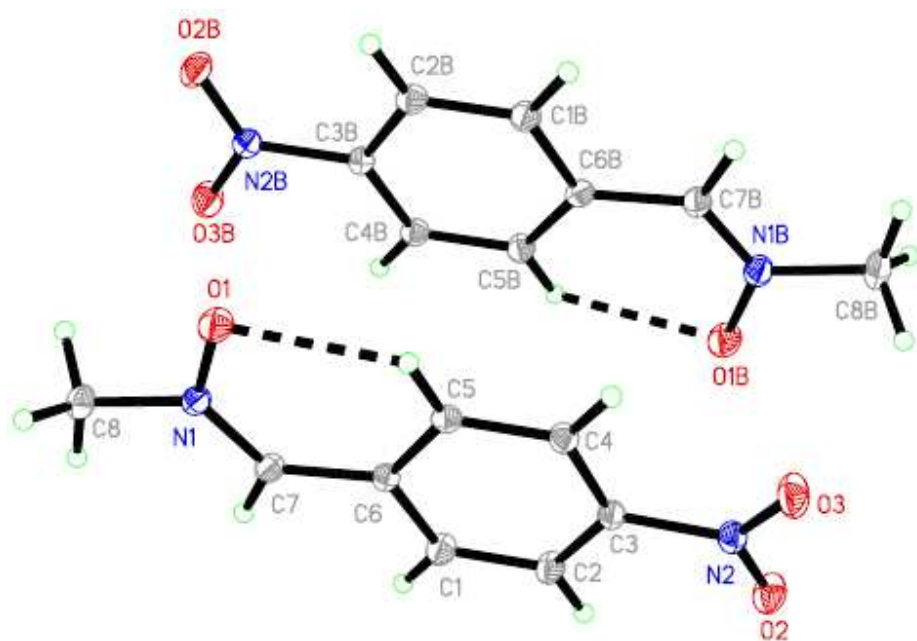


Fig. 2. ORTEP drawing of (*Z*)-*N*-methyl-*C*-4-nitrophenyl nitrone **Z-2b** showing the atom numbering scheme and 30% probability displacement ellipsoids of non-H atoms.

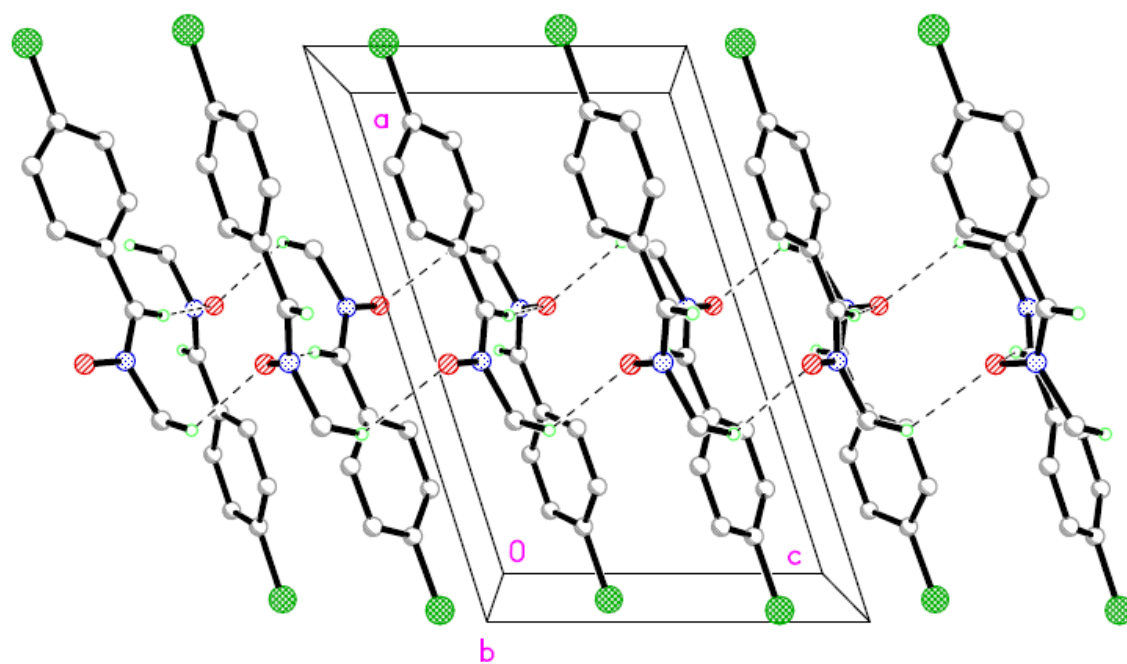


Fig. 3. Packing diagram for (*Z*)-*N*-methyl-*C*-4-chlorophenyl nitrone **Z-2a**, viewed down the *b* axis.

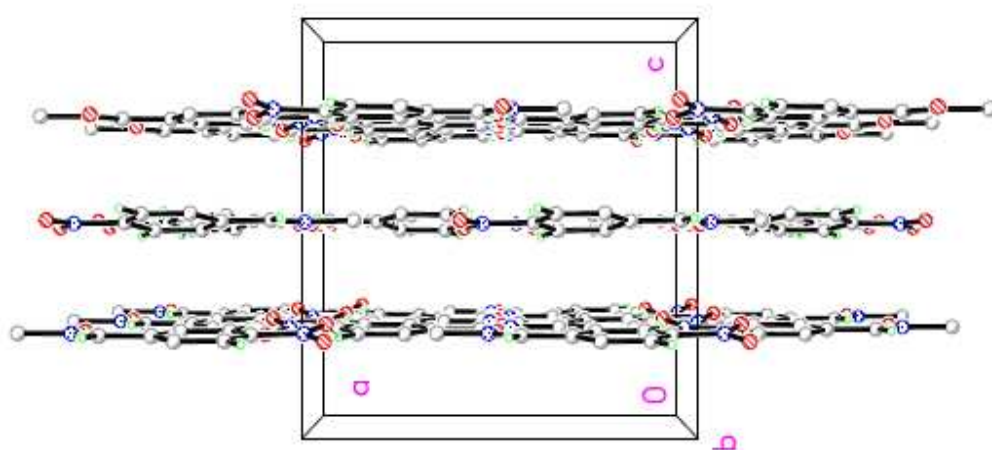


Fig. 4. Packing diagram for (*Z*)-*N*-methyl-*C*-4-nitrophenyl nitrone **Z-2b**, viewed down the *b* axis.

3.2. Computational study

3.2.1. Geometry optimization

The structures of *Z/E* 4-substituted phenyl nitrones **Z-2a**, **E-2a**, **Z-2b**, **E-2b**, **Z-2c** and **E-2c** were optimized using DFT at the B3LYP/6-311++G(d,p) level of theory. Selected bond lengths, bond and torsion angles of the experimental and calculated data (gas-phase), DFT (B3LYP/6-311++G(d,p)), are shown in in Table 2. It is showed that obtained optimized parameters have a good correlation with X-ray results. All bonds lengths as similar as experimental data for **Z-2a** and **Z-2b**. However, H-C bonds in optimized structure are longer than that in crystal structure (longer by 0.13 Å). In **Z-2a**, the most notable inconsistency occurs at C-N-C-C torsion angle (176.85° for X-ray, 179.99° for DFT) and O-N-C-C torsion angle (-0.01° for X-ray, -2.04° for DFT). In **Z-2b**, the most notable inconsistency occurs at C-N-C-C torsion angle (-179.77° for X-ray, 0.00° for DFT) and O-N-C-C torsion angle (-1.016° for X-ray, 0.01° for DFT). All of

these torsion angles are partially involved in the hydrogen bond. It can be considered that intermolecular interaction affects the crystal system [22]. Comparing the structural parameters for the three pairs of isomers showed that there are a difference in torsion angles C-N-C-C and O-N-C-C for **Z-2a**, **E-2a**, **Z-2b**, **E-2b**, **Z-2c** and **E-2c** about 6.0° and 4.0°, respectively. This difference attributed to the twisting of *E*-isomers.

Table 2. Selected structural parameters for *Z/E*-isomers

Atomic numbering	Z-2a	E-2a	Exper.	Z-2b	E-2b	Exper.	Z-2c	E-2c
C(C ₆ H ₄)-C (Å)	1.45	1.46	1.45	1.45	1.45	1.45	1.45	1.46
C-H (Å)	1.08	1.08	0.95	1.08	1.08	0.95	1.08	1.08
C-N (Å)	1.32	1.32	1.31	1.32	1.32	1.31	1.32	1.31
N-O (Å)	1.28	1.28	1.29	1.27	1.27	1.29	1.28	1.28
N-C (CH ₃) (Å)	1.48	1.48	1.47	1.48	1.48	1.47	1.48	1.48
C-N-C-C (°)	179.99	-6.49	176.85	0.00	-6.74	-179.77	179.99	-6.54
O-N-C-C (°)	-0.01	175.87	-2.04	0.01	175.93	-1.016	0.00	175.61

3.2.2 Vibrational and potential energy distribution (PED) analysis

The assignment of the fundamental vibrations of the optimized ground state geometry of **Z-2a**, **Z-2b** and **Z-2c** reported at the B3LYP/6-311++G(d,p) level using Gaussian 09 program. Vibration frequencies calculated at B3LYP/6-311++G(d,p) level were scaled by 0.9679, which is a typical scaled factor for the calculated method [23]. The detailed

descriptions of the assignment have been shown in Table 3, Table S1 and Table S2 (Supplementary Information). Veda 4 software [21] was used to assign the calculated frequencies. The predicted vibration frequencies and the experimental data are very close to each other. In conclusion, the scaled frequencies of the DFT calculation are in good agreement with the corresponding FTIR vibration.

Table 3. Computational calculated vibrational wavenumbers (harmonic frequency (cm^{-1})), assignments and contribution for (*Z*)-*N*-methyl-*C*-4-chlorophenyl nitron **Z-2a** at DFT/B3LYP utilizing 6-311++G (d,p) basis sets.

Frequencies		PED (%)						
Experimental	DFT							
3183	3134	υ CH 97						
3085	3105	υ CH 96						
	3100	υ CH 94						
	3096	υ CH 97						
3038	3064	υ CH 95						
3038	3052	υ CH -17	υ CH -16	υ CH 65				
	3041	υ CH -50	υ CH 50					
2946	2961	υ CH 33	υ CH 33	υ CH 33				
1595	1580	υ NC 47						
1556	1573	υ CC 25	υ CC -11	β CCC - 10				
1485	1538	υ CC -24	υ CC 10	υ CC 23				

1427	1467	β HCC 15	β HCC 14	β HCC - 13				
1427	1455	β HCC 14	β HCH 12	β HCH - 24	β HCH 12	τ HCNC 10	τ HCNC -10	
	1420	β HCH -39	β HCH 39	τ HCNC 13				
1405	1413	υ ON 22	β HCC 25	β HCH 25				
	1387	β HCH -18	β HCH - 11	β HCH - 17				
	1381	υ CC 10	υ CC -15	β HCC - 12				
1310	1297	υ CC 10	υ CC 20	β HCC 10	β HCC 17			
1257	1279	υ CC -14	υ CC 19	β HCC 11	β HCC - 10	β HCC 16		
	1208	υ CC -16	υ CC 27	β CCC - 12				
1162	1166	υ ON -10	β HCC 12	β HCC 24				
	1157	υ ON 35	υ NC -11	β HCC - 13	β HCC -10			
	1101	υ CC -11	υ CC 10	β HCC - 14	β HCC 21	β HCC - 12	β HCC -12	
1090	1100	β HCH 16	β HCH - 16	τ HCNC - 52				

	1068	β HCH -10	τ HCNC 20	τ HCNC - 20				
	1062	υ CC 16	υ CC 18	υ CIC -12	τ HCNC 10			
1013	992	β CCC -41	β CCC - 22	β CCC 19				
950	967	τ HCCC 54	τ HCCC 27	τ CCCC 10				
	941	υ ON 19	υ NC 36	β NCC - 11				
	933	τ HCCC 25	τ HCCC - 41	τ CCCC 13				
856	840	υ CC -17	υ CC -12	β CCC - 18				
	830	τ HCCC - 30	τ HCCC 42					
	811	τ HCCC - 14	τ HCCC 38	τ HCCC 30				
	768	τ HCCC 62	τ HCCC 12					
706	708	τ CCCC - 18	τ CCCC - 28	γ CCCC - 17				
	693	υ NC -13	υ CIC -19	β CCC - 17				
630	625	β CCC -12	β CCC - 20	β CCC 33				

	581	γ OCCN - 59						
	557	υ NC 16	υ CIC -13	β ONC 37				
	492	τ HCCC 11	γ OCCN 16	γ CICC - 18	γ CCCC 30			
	449	υ CIC 30	β ONC 29	β CNC - 11				
	409	τ HCCC 12	τ CCCC - 37	τ CCCC - 24	τ CCCC 16			
	363	β CCC -30	β CNC 18	β CICC 26				
	344	τ CCCC 22	τ CNCC - 17	γ CICC - 29				
	293	υ CC 15	υ CIC 14	β CCC 14	β CNC 25			
	263	β NCC 23	β CICC 41					
	187	τ HCNC 20	τ CNCC 22	γ CICC - 25				
	142	τ HCNC 25	τ HCNC 25	τ CNCC - 17				
	136	β NCC -28	β CCC 38	β CICC 12				
	79	τ NCCC 59	τ CNCC 22					

	61	τ NCCC - 13	τ CCCC - 14	τ CCCC 25	τ CNCC 13	γ CCCC -20	
--	----	---------------------	---------------------	-------------------	-------------------	-------------------	--

ν – stretching; γ – out-of-plane deformation; τ – torsion; β – bending.

Aromatic C–H vibrations

Weak bands in the region $3100\text{--}3000\text{cm}^{-1}$ in aromatic compounds are assigned to aromatic C–H stretching vibrations [24]. For the compound **Z-2a**, the C–H stretching vibrations are found at 3080 (m) and 3036 (m) [DFT: $3134\text{--}3064\text{ cm}^{-1}$], for the compound **Z-2b**, the C–H stretching vibrations are found at 3080 (w) [DFT: $3121\text{--}3080\text{ cm}^{-1}$], For the compound **Z-2c**, the C–H stretching vibrations are overlap with water broad bands [DFT: $3129\text{--}3091\text{ cm}^{-1}$], The theoretically computed C–H vibrations shows good agreement with recorded spectrum as well as the literature data [24].

The presence in the IR spectra of a strong band ν C–H near 3100 cm^{-1} is a characteristic feature of cyclic aldo-nitrones [25]. This peak appeared at 3185 cm^{-1} [DFT: 3105 cm^{-1}] and 3112 cm^{-1} [DFT: 3095 cm^{-1}] for compounds **Z-2a** and **Z-2b**, respectively. This peak is overlapped with water broad bands [DFT: 3101 cm^{-1}] in compound **Z-2c**.

C–C vibrations

The ring stretching vibrations of benzene and their derivatives are highly characteristic of the aromatic ring itself. The bands between 1400 and 1650 cm^{-1} in benzene derivatives are usually assigned to C–C stretching modes [26]. For the compound **Z-2a**, the C–C stretching vibrations are found at 1592 (s), 1555 (s), and 1484 (s) [DFT: 1573 and 1538 cm^{-1}], for the compound **Z-2b**, the C–C stretching vibrations are found at 1598 (s), 1577 (m), and 1510 (s) [DFT: 1583, 1579, 1553 and 1517 cm^{-1}], for the compound **Z-2c**, the C–C stretching vibrations are found at 1603 (s), 1569 (s), 1509 (s) and 1414 (s) cm^{-1} [DFT: 1593, 1583, 1544 and 1400 cm^{-1}], the mean difference between theoretical (B3LYP/6-311++G(d,p)) and experimental frequencies are acceptable. It shows the good agreement between theoretical and experimental C–C stretching vibrations.

Methyl group (C–H) vibrations

The C–H methyl group stretching vibrations are generally observed in the range 3000–2800 cm^{-1} [26]. In the compound **Z-2a**, the bands with medium peaks assigned for the CH_3 stretching vibrations are found at 2944 (m) cm^{-1} [DFT: 3059 cm^{-1}], for the compound **Z-2b**, the C–H stretching vibrations are found at 3012 (m) cm^{-1} [DFT: 3063 cm^{-1}], for the compound **Z-2c**, the C–H stretching vibrations are found at 2946 (s) cm^{-1} [DFT: 3055 cm^{-1}]. The theoretical calculations overestimate the experimental data by about 3%. In addition to methyl group, the compound **Z-2c** has a methoxy group (OCH_3), the C–H of methoxy appeared at 2841 cm^{-1} [DFT: 3008 cm^{-1}].

C–N and O–N vibrations

The C–N and O–N stretching vibrations are the main characteristic IR bands of a nitro compound and occur at about 1520–1590 and 1200–1350 cm^{-1} , respectively [27]. The C–N and O–N stretching for the compound **Z-2a** are found at 1592 (s) and 1308 (s), respectively [DFT: 1580 and 1413 cm^{-1} , respectively], for the compound **Z-2b**, the C–N and O–N stretching vibrations are found at 1598 (s) and 1341 cm^{-1} (s), respectively [DFT: 1553 and 1316 cm^{-1} , respectively], for the compound **Z-2c**, the C–N and O–N stretching vibrations are found at 1603 (s) and 1341 cm^{-1} (s), respectively [DFT: 1593 and 1411 cm^{-1} , respectively]. The mean difference between theoretical (B3LYP/6-311++G(d,p)) and experimental frequencies are acceptable. It shows the good agreement between theoretical and experimental C–N and O–N stretching vibrations.

In conclusion, the theoretical calculation of vibrations frequencies at B3LYP/6-311++G(d,p) method approximately coincides with observed values of FTIR and these assignments are in good agreement with the literature data [24-27].

3.2.3. NMR Analysis

The ^1H and ^{13}C NMR spectra of the (*Z*)-*N*-methyl-*C*-4-substituted phenyl nitrones **Z-2a**, **Z-2b** and **Z-2c** were recorded experimentally in deuterated chloroform (CDCl_3) as well as they have been calculated using DFT/B3LYP/6-311++G(d, p) level of theory with GIAO approach in chloroform. The chemical shifts for ^1H and ^{13}C nuclei in solution and theoretical values are collected and reported in Table 4. Chemical shifts in the ^1H and ^{13}C NMR spectra were assigned with the help of DFT calculations of shielding constants. The obtained shielding constants were recalculated into theoretical chemical shifts. For this purpose the TMS shielding constants were calculated at the same level of theory as for acyclic nitrones **Z-2a**, **Z-2b** and **Z-2c**. The theoretically calculated chemical shifts were in good agreement with the experimental ones, and the correlation coefficients for ^1H were 0.9643 (**Z-2a**), 0.9424 (**Z-2b**) and 0.971 (**Z-2c**). The correlation coefficients for ^{13}C were 0.9903 (**Z-2a**), 0.9966 (**Z-2b**) and 0.9957 (**Z-2c**) (Fig. S1). The effect of the electron withdrawing chloro and nitro groups and the electron donating methoxy group on chemical shifts can be seen in quaternary carbon C-9 of the phenyl ring, with experimental chemical shifts of 135.6, 147.9 and 161.1 ppm in **Z-2a**, **Z-2b** and **Z-2c**, respectively. This trend also observed in theoretical results.

Table 4. Comparison of the calculated chemical shifts (GIAO B3LYP/6-311++G(d,p)) with experimental in CDCl_3 .

Atom	Z-2a		Z-2b		Z-2c	
	Exp	DFT-TMS	Exp	DFT-TMS	Exp	DFT-TMS
H-4	7.28	7.61	7.54	7.81	7.25	7.49
H-6	8.09	9.81	8.4	9.84	8.14	9.87
H-8	7.28	7.69	8.4	8.66	6.86	7.03
H-11	7.28	7.59	8.28	8.54	6.86	7.20
H-13	7.28	7.38	8.28	7.48	6.86	7.36

H-15	3.77	3.77	3.98	3.86	3.75	3.71
H-16	3.77	3.77	3.98	3.86	3.75	3.71
H-17	3.77	3.67	3.98	3.80	3.75	3.59
H	-	-	-	-	3.76	3.83
H	-	-	-	-	3.76	3.83
H	-	-	-	-	3.76	4.15
C-2	129.5	137.6	136	145.7	123.4	131.5
C-3	134	142.6	133.1	142.7	135.2	142.8
C-5	128.6	134.9	128.7	133.0	130.5	136.2
C-7	128.9	135.8	123.8	132.7	113.8	114.2
C-9	135.6	151.3	147.9	155.4	161.1	170.2
C-10	128.9	134.9	123.8	130.9	113.8	123.6
C-12	128.6	137.4	128.7	136.0	130.5	138.3
C-14	54.4	57.8	55.1	58.9	53.8	57.0
C-15	-	-	-	-	55.3	57.7

3.2.4. Thermodynamic study

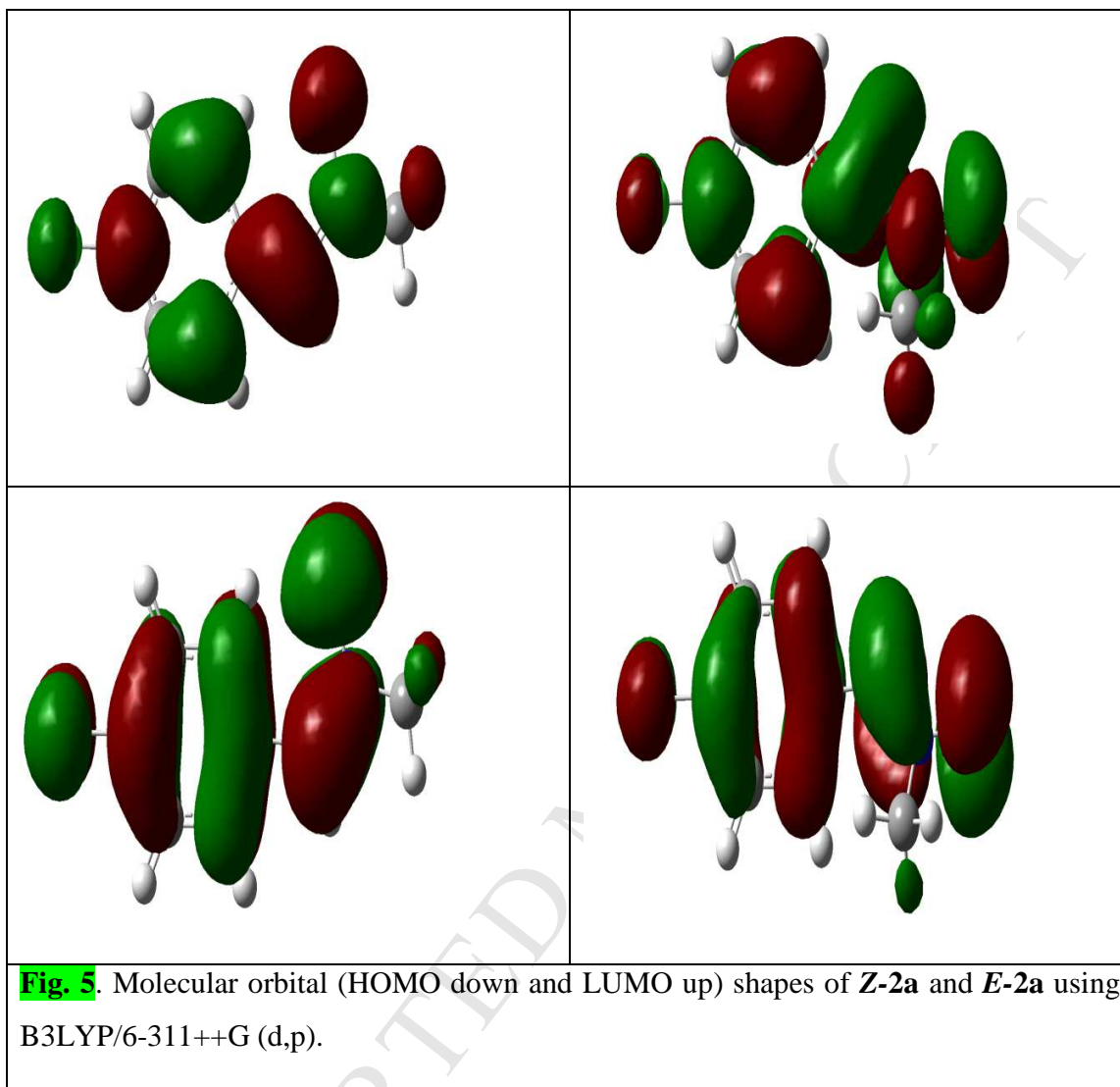
Z- and *E*-isomers of the three compounds were studied using theoretical calculation to evaluate the energetic difference between both isomers and the relative importance of the intramolecular hydrogen bonds. Thermodynamics study showed that the *Z*-isomer is favoured than *E*-isomer with energy barrier of 7.1, 7.2 and 7.1 Kcal/mol for **Z-2a**, **Z-2b** and **Z-2c**, respectively, this value is consistent with breaking of intramolecular H bond N—O...H. The relative abundances of the *Z*- and *E*-isomers were calculated using Gibbs free energy equation; $\Delta G = -RT \ln K$ (where ΔG denotes the difference between the Gibbs

free energies of *E*-isomer relative to the *Z*-isomer and *K* is the corresponding equilibrium constant). The abundance of the most stable species, *Z* is equal to 99.99% for all three compounds at 298 K in gas phase. This indicates that the *Z*-isomer is the predominant in the gas phase. These results are in good agreement with the experimentally measured X-ray structure and NMR spectra which showed a pure single *Z*-isomer as well as in agreement with the literature [28].

3.2.5. Molecular Orbital analysis

Frontier molecular orbitals (FMOs) play crucial role in the chemical stability of a molecule and in the interactions between atoms. They are considered to be effective in determining the characteristics of the molecules such as optical properties and biological activities. Among these, the highest occupied molecular orbital (HOMO) and the lowest unoccupied molecular orbital (LUMO) are the most important. The HOMO represents the ability of a molecule to donate an electron, while the LUMO is an electron acceptor. Fig. 5, Fig. S2 and Fig. S3 (Supplementary Information) show the electron density in HOMO and LUMO molecular orbitals. In (*Z*)-*N*-methyl-*C*-4-chlorophenyl nitrone **Z-2a** and (*E*)-*N*-methyl-*C*-4-chlorophenyl nitrone **E-2a**, the HOMO and LUMO orbitals were mainly delocalized over the molecule with high electron density on nitrogen atoms in HOMO which reduced in LUMO suggesting $n-\pi^*$ transition, HOMO showed π -bonding over whole molecule, whereas LUMO showed π^* -antibonding on the molecule, suggesting $\pi-\pi^*$, therefore, the transitions from HOMO to LUMO are mixture of $\pi-\pi^*$ and $n-\pi^*$.

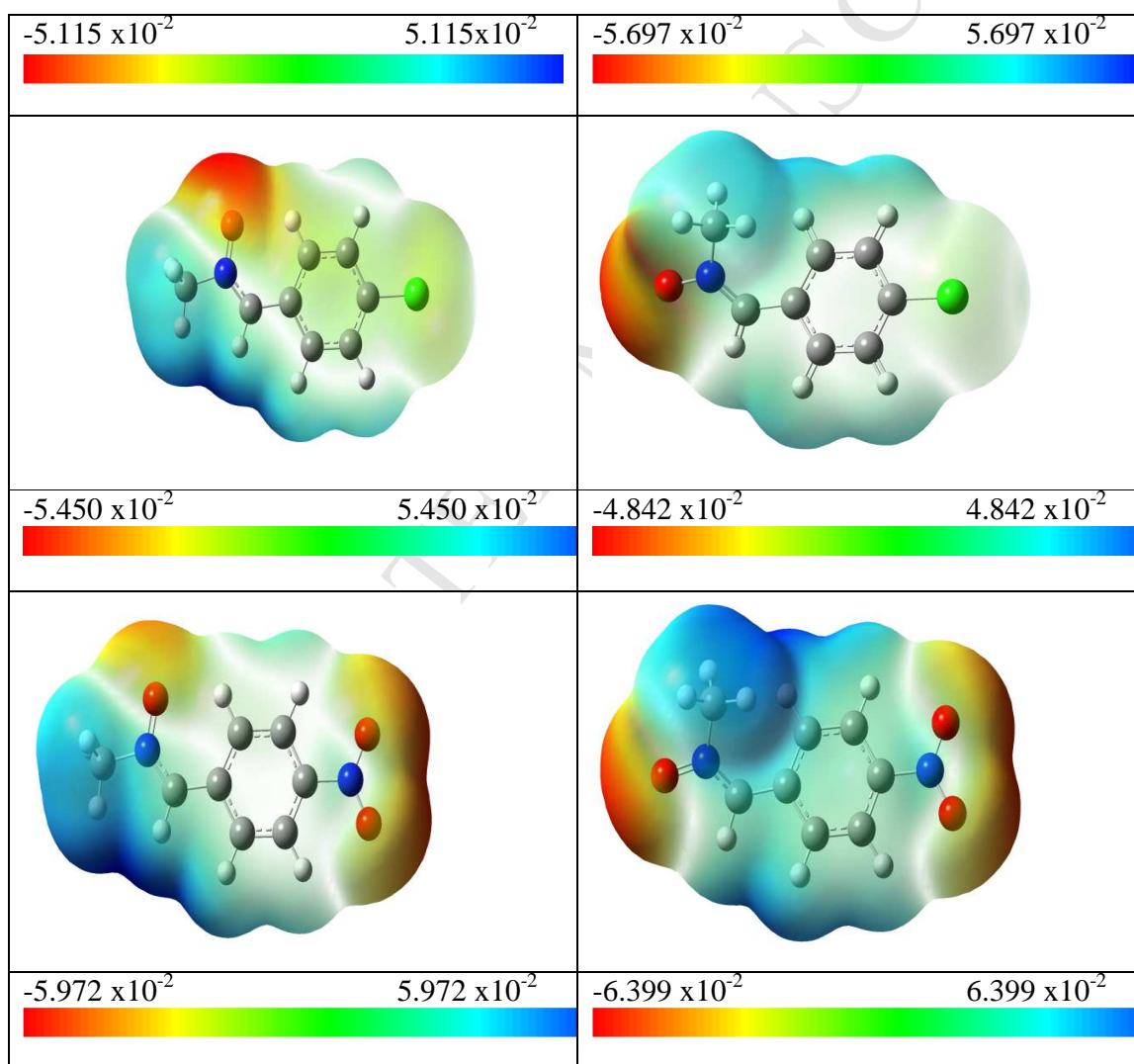
Z-2a	E-2a
-------------	-------------

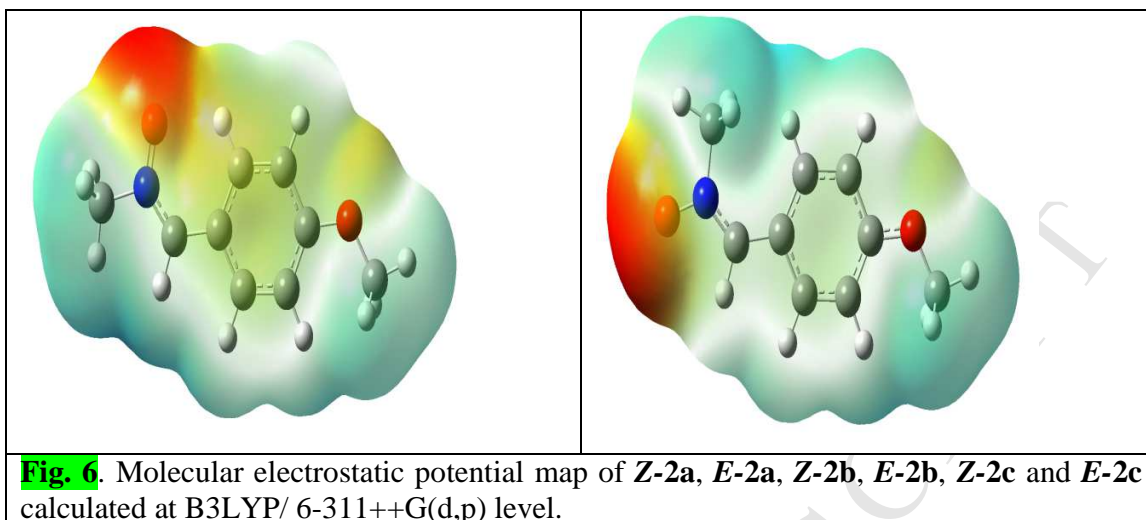


3.2.6. Molecular electrostatic potential

Molecular electrostatic potential (MEP) is used for investigating the chemical reactivity of a molecule, the surfaces of *Z-2a*, *E-2a*, *Z-2b*, *E-2b*, *Z-2c* and *E-2c* were plotted over an optimized electronic structures using B3LYP/6-311++G(d,p) as shown in Fig. 6. The MEP is especially important for the identification of the reactive sites of nucleophilic or electrophilic attack in hydrogen-bonding interactions and for the understanding of the process of biological recognition. The most positive (blue) regions are localized on hydrogen atoms of azomethine group ($C(H)=N$), showing electrophilic reactivity; whereas the most negative (red) regions are observed around the oxygen atoms. The MEP

map is supported by the intermolecular interactions, C8—H8...O1 [symmetry code: $1-x, 1/2+y, 3/2-z$] and C7—H7...O1 [$x, 1/2 - y, -1/2 + z$] hydrogen bonds, which linked the molecules into supramolecular chains propagating along the *b* axis direction (Fig. 3) for compound **Z-2a**. The crystal structure of compound **Z-2b** also supported the MEP; molecules are linked through intermolecular C7—H7A...O1 [symmetry code: $1-x, 1/2+y, z$], C2—H2A...O3 [symmetry code: $-x, 1/2+y, z$] and C4—H4A...O2 [symmetry code: $-x, -1/2+y, z$].





Conclusions

In this work, (*Z*)-*N*-methyl-*C*-4-chlorophenyl nitrone **Z-2a**, (*Z*)-*N*-methyl-*C*-4-nitrophenyl nitrone **Z-2b** and (*Z*)-*N*-methyl-*C*-4-methoxyphenyl nitrone **Z-2c** were synthesized by treatment of 4-chlorobenzaldehyde, 4-nitrobenzaldehyde or 4-methoxybenzaldehyde, respectively, with *N*-methylhydroxylamine and sodium carbonate. The geometries of the **Z-2a**, **Z-2b** and **Z-2c** and their *E*-isomers; (*E*)-*N*-methyl-*C*-4-chlorophenyl nitrone **E-2a**, (*E*)-*N*-methyl-*C*-4-nitrophenyl nitrone **E-2b** and (*E*)-*N*-methyl-*C*-4-methoxyphenyl nitrone **E-2c** molecules were optimized using DFT at the B3LYP/6-311++G(d,p) level of theory. The theoretical vibrational frequencies obtained by DFT calculations are in good agreement with the experimental values. The electronics structures were described in terms of the distribution of the HOMO and LUMO. GIAO method was used to calculate the NMR spectra, the correlation between the calculated and experimental chemical shifts is mostly in the range of 0.94-0.97 for ^1H , whereas, the correlation for ^{13}C is 0.99. Thermodynamic study showed that the *Z*-isomer is favoured than *E*-isomer with energy barrier of 7.1, 7.2 and 7.1 Kcal/mol for **Z-2a**, **Z-2b** and **Z-2c**, respectively. The abundance of the most stable *Z*-isomers is equal to 99.99% for all three compounds at 298 K in gas phase. MEP shows that the most positive (blue) regions are localized on hydrogen atoms of azomethine group ($\text{C}(\text{H})=\text{N}$), showing electrophilic reactivity; whereas the most negative (red) regions are observed around the oxygen

atoms. Moreover, these results are supported by crystal structure packing of compounds **Z-2a** and **Z-2b**.

Acknowledgment

This project was funded by the Deanship of Scientific Research (DSR) at King Abdulaziz University, Jeddah, under grant no. (G-100-662-37). The authors, therefore, acknowledge with thanks DSR for technical and financial support.

Appendix A. Supplementary material

Supplementary data associated with this article can be found, in the online version, at...

References

- [1] L. Smith, Chem. Rev. 23 (1938) 193.
- [2] J. Hamer, A. Macaluso, Chem. Rev. 64 (1964) 473.
- [3] A. Padwa, W.H. Pearson, Synthetic Application of 1,3,-Dipolar Cycloaddition Chemistry Toward Heterocycles and Natural Products, Wiley, New Jersey, 2003.
- [4] (a) J. Lasri, S.M. Soliman, M.A. Januário Charmier, M. Ríos-Gutiérrez, L.R. Domingo, Polyhedron 98 (2015) 55; (b) J. Lasri, Polyhedron 57(2013) 20; (c) R.R. Fernandes, J. Lasri, M.F.C. Guedes da Silva, A.M.F. Palavra, J.A.L. da Silva, J.J.R. Fraústo da Silva, A.J.L. Pombeiro, Adv. Synth. Catal. 353 (2011) 1153; (d) J. Lasri, M.F.C. Guedes da Silva, M.N. Kopylovich, S. Mukhopadhyay, M.A. Januário Charmier, A.J.L. Pombeiro, Dalton Trans. (2009) 2210; (e) M.N. Kopylovich, J. Lasri, M.F.C. Guedes da Silva, A.J.L. Pombeiro, Dalton Trans. (2009) 3074; (f) J. Lasri, M.N. Kopylovich, M.F.C. Guedes da Silva, M.A. Januário Charmier, A.J.L. Pombeiro, Chem. Eur. J. 14 (2008) 9312; (g) J. Lasri, M.A. Januário Charmier, M. Haukka, A.J.L. Pombeiro, J. Org. Chem. 72 (2007) 750.
- [5] R.A. Floyd, R.D. Kopke, C.-H. Choi, S.B. Foster, S. Doblás, R.A. Towner, Free Radical. Biol. Med. 45 (2008) 1361.
- [6] A. Herbrechtsmier, F.-M. Schnepel, O. Glemser, J. Mol. Struct. 50 (1978) 43.

- [7] N.S. Ferris, W.H. Woodruff, D.B. Rorabacher, T.E. Jones, L.A. Ochrymocyocz, J. Am. Chem. Soc. 100 (1978) 5939.
- [8] R.A. Floyd, H.K. Chandru, T. He, R. Towner, Anticancer Agents Med Chem. 11 (2011) 373.
- [9] C.H. Choi, K. Chen, A. Vasquez-Weldon, R.L. Jackson, R.A. Floyd, R.D. Kopke, Free Radical Biol. Med. 44 (2008) 1772.
- [10] I.A. Sekine, A. Masuko, K. Senoo, Corros. Sci. 43 (1987) 553.
- [11] M.A. Quarishi, D. Jamal, Corros. Sci. 56 (2000) 156.
- [12] E. Heitz, Advances in Corrosion Science and Technology, Plenum Press, New York, NY, 1974. vol. 4.
- [13] M.Z.A. Rafiquee, S. Khan, N. Saxena, M.A. Quarishi, Port. Spectrochim. Acta 25 (2007) 419.
- [14] Z. Otwinowski, W. Minor, Processing of X-ray Diffraction Data Collected in Oscillation Mode, Academic Press, New York, pp. 307-326, 1997. In Methods in Enzymology, Volume 276, Macromolecular Crystallography, Part A, C.W. Carter, J. Sweet, Eds.; Academic Press: New York, USA, 1997; pp 307-326.
- [15] Agilent, CrysAlisPro, Agilent Technologies inc., 2013, Yarnton, Oxfordshire, England.
- [16] L. Palatinus, G. Chapuis, J. Appl. Cryst. 40 (2007) 786.
- [17] G.M. Sheldrick, SADABS - Bruker AXS scaling and absorption correction -, Bruker AXS, Inc., Madison, Wisconsin, USA, 2012.
- [18] G.M. Sheldrick, Acta Cryst. A64 (2008) 112.
- [19] Gaussian 09, Revision A.02, M.J. Frisch, G.W. Trucks, H.B. Schlegel, G.E. Scuseria, M.A. Robb, J.R. Cheeseman, G. Scalmani, V. Barone, B. Mennucci, G.A. Petersson, H. Nakatsuji, M. Caricato, X. Li, H.P. Hratchian, A.F. Izmaylov, J. Bloino, G. Zheng, J.L. Sonnenberg, M. Hada, M. Ehara, K. Toyota, R. Fukuda, J. Hasegawa, M. Ishida, T. Nakajima, Y. Honda, O. Kitao, H. Nakai, T. Vreven, J.A. Montgomery, Jr., J.E. Peralta, F. Ogliaro, M. Bearpark, J.J. Heyd, E. Brothers, K.N. Kudin, V.N. Staroverov, R. Kobayashi, J. Normand, K. Raghavachari, A. Rendell, J.C. Burant, S.S. Iyengar, J. Tomasi, M. Cossi, N. Rega, J.M. Millam, M. Klene, J.E. Knox, J.B. Cross, V. Bakken, C. Adamo, J. Jaramillo, R. Gomperts, R.E. Stratmann, O. Yazyev, A.J. Austin, R. Cammi,

C. Pomelli, J.W. Ochterski, R.L. Martin, K. Morokuma, V.G. Zakrzewski, G.A. Voth, P. Salvador, J.J. Dannenberg, S. Dapprich, A.D. Daniels, O. Farkas, J.B. Foresman, J.V. Ortiz, J. Cioslowski, D.J. Fox, Gaussian, Inc., Wallingford CT, 2009.

[20] Chemcraft software, <http://www.chemcraftprog.com>.

[21] M.H. Jamroz, Vibrational Energy Distribution Analysis VEDA 4, Warsaw, 2004-2010.

[22] H. Bülbül, Y. Köysal, N. Dege, S. Gümüş, E. Açar, J. Crystallogr. 2015 (2015) 6.

[23] M.P. Andersson, P. Uvdal, J. Phys. Chem. A 109 (2005) 2937.

[24] S. Ramalingam, S. Periandy, M. Govindarajan, S. Mohan, Spectrochim Acta A Mol. Biomol. Spectrosc. 75 (2010) 1308.

[25] Nitrile Oxides, Nitrones, and Nitronates in Organic Synthesis. Novel Strategies in Synthesis. Second Edition, H. Feuer. Ed., John Wiley & Sons, Inc. Hoboken, New Jersey, 2008.

[26] A. Suvitha, S. Periandy, S. Boomadevi, M. Govindarajan, Spectrochim Acta A Mol. Biomol. Spectrosc. 117 (2014) 216.

[27] A. Padwa, Science of Synthesis: Houben-Weyl Methods of Molecular Transformations Vol. 27: Heteroatom Analogues of Aldehydes and Ketones. Georg Thieme Verlag, 2014, 1174 pages.

[28] J. Lasri, A.I. Ismail, M. Haukka, S.M. Soliman, Spectrochim Acta A Mol. Biomol. Spectrosc. 136 (2015) 1857.

Highlights

- Crystal structures of (*Z*)-*N*-methyl-*C*-4-substituted phenyl nitrones were described.
- IR and NMR spectra of (*Z*)-*N*-methyl-*C*-4-substituted phenyl nitrones were studied.
- DFT calculations were used to assign the NMR chemical shifts.
- DFT calculations were used to analyze the molecular orbitals and molecular electrostatic potential.
- Correlation between experimental and computational spectroscopy was evaluated.
- Thermodynamic study of isomerism was reported.